SUPPLEMENTAL INFORMATION

Modulation of redox metabolism negates cancer-associated fibroblasts-induced treatment resistance in a heterotypic 3D culture platform of pancreatic cancer

Mans Broekgaarden[1], Sriram Anbil[1,2#], Anne-Laure Bulin[1#], Girgis Obaid[1#], Zhiming Mai[1], Yan Baglo[1], Imran Rizvi[1], Tayyaba Hasan[1,3]*.

1. *Wellman Center for Photomedicine, Department of Dermatology, Massachusetts General Hospital, Harvard Medical School, Boston MA.*
2. *The University of Texas School of Medicine at San Antonio*
3. *Division of Health Sciences and Technology, Harvard-Massachusetts Institute of Technology, Boston MA.*

* Corresponding author:
Prof. Tayyaba Hasan.
Wellman Center for Photomedicine, Massachusetts General Hospital
Department of Dermatology, Harvard Medical School
40 Blossom Street, 02114 Boston, MA.
Tel: 617-726-6856.
Fax: 617-726-8566.
E-mail: t.hasan@mgh.harvard.edu.

# Equal contributions

Table S1: Latest mycoplasma test prior to the completion of the experimental work of this manuscript. Test performed on June 22, 2017, cell culture experiments concluded on July 30, 2017. Luminescence is measured before (reading A, background) and after addition of MycoAlert mycoplasma detection substrate (reading B). A/B ratios higher >1.2 are considered mycoplasma positive.

Cell culture	Neg. Ctrl	MP2	AsPC-1	HDF1	HDF2	CAF1	CAF6
Ratio	0.49	0.34	0.69	0.54	0.70	0.28	0.98

Figure S1.

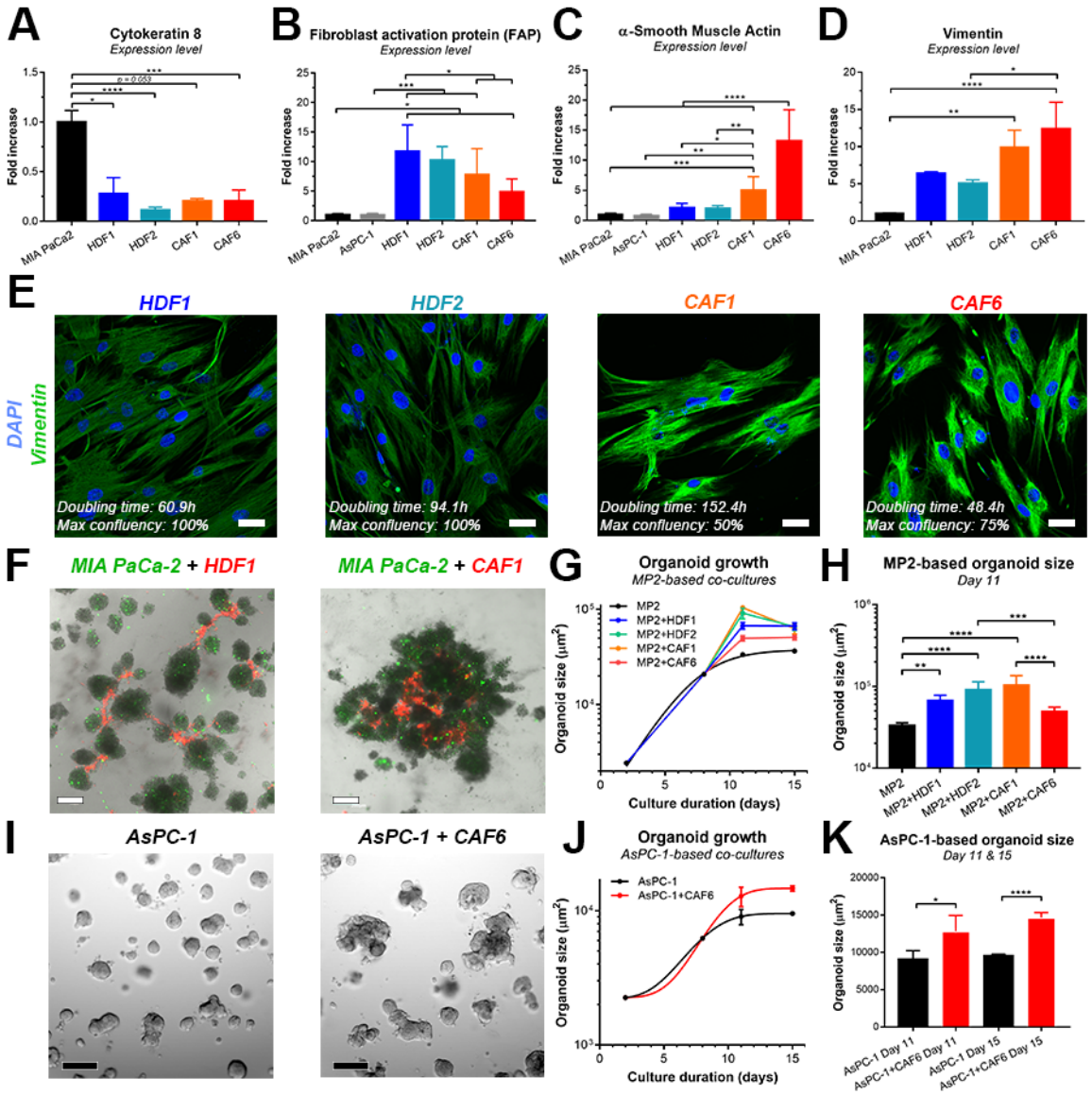

Figure S1: Molecular characterization of the various patient-derived fibroblasts. (A-D) Quantification of CK8 **(A)**, FAP **(B)**, α-SMA **(C)**, and vimentin **(D)** expression levels in the cancer cell and fibroblast monolayer cultures (mean ± SD of N = 6-9, normalized to MP2). **(E)** Morphological characterization of fibroblasts in culture following staining with DAPI (nucleus, blue) and Vimentin (green). Scalebar = 50 µm. **(F)** Fluorescence microscopy images depicting MP2 microtumors (stained with DiO, green) and either HDF1 or CAF1 cells (stained with DiD, red). Scalebar = 200 µm. **(G)** Growth of MP2-based microtumor co-cultures (mean ± SEM of N = 4000). **(H)** Size of MP2-based microtumor co-cultures (mean ± 95% CI). (I) Brightfield microscopy images of AsPC-1 and AsPC-1+CAF6 microtumor cultures. Scalebar = 200 µm. **(J)** Growth of AsPC-1-based microtumor co-cultures (mean ± SEM of N = 100-4000). (K) Size of AsPC-1-based microtumor co-cultures. Data depicts the mean ± 95% CI.

Figure S2.

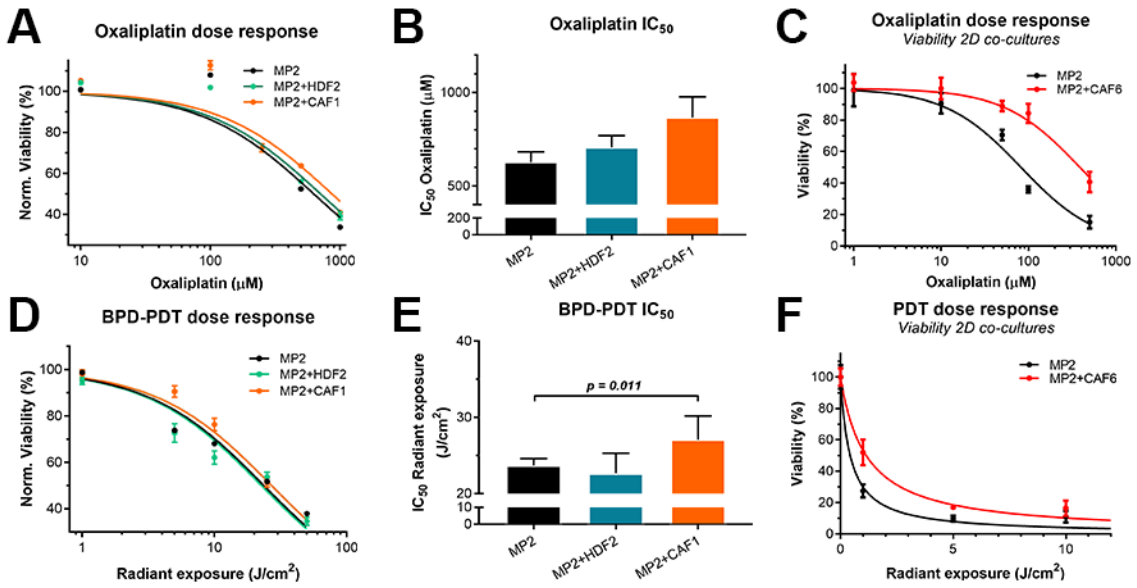

Figure S2. MP2 microtumors co-cultured with cancer associated fibroblasts (CAF1) exhibit reduced treatment sensitivity to BPD-PDT and oxaliplatin chemotherapy. (A) Oxaliplatin dose-response curves based on normalized median viability. Depicted are the mean ± SD of N = 12-60 measurements obtained from 4 technical repeats. **(B)** Comparison of the fitted oxaliplatin IC_{50} doses between MP only (black), MP2+HDF2 (turquoise), and MP2+CAF1 (orange) cultures, extracted from the dose-response data in panel (A), N = 128-184 x-values. **(C)** Oxaliplatin dose response curves obtained from MP2 (black) and MP2+CAF6 (red) 2D (co)cultures (mean ± SD of N = 4-8). **(D)** BPD-PDT radiant exposure dose-response curves based on normalized median viabilities. Depicted are the mean ± SD of N = 12-60 measurements obtained from 4 technical repeats. **(E)** Comparison of the fitted radiant exposure IC_{50} doses between MP only (black), MP2+HDF2 (turquoise), and MP2+CAF1 (orange) cultures, extracted from the dose-response data in panel (D), N = 144-204 x-values. **(F)** BPD-PDT radiant exposure dose response curves obtained from MP2 (black) and MP2+CAF6 (red) 2D (co)cultures (mean ± SD of N = 4-8).

Figure S3.

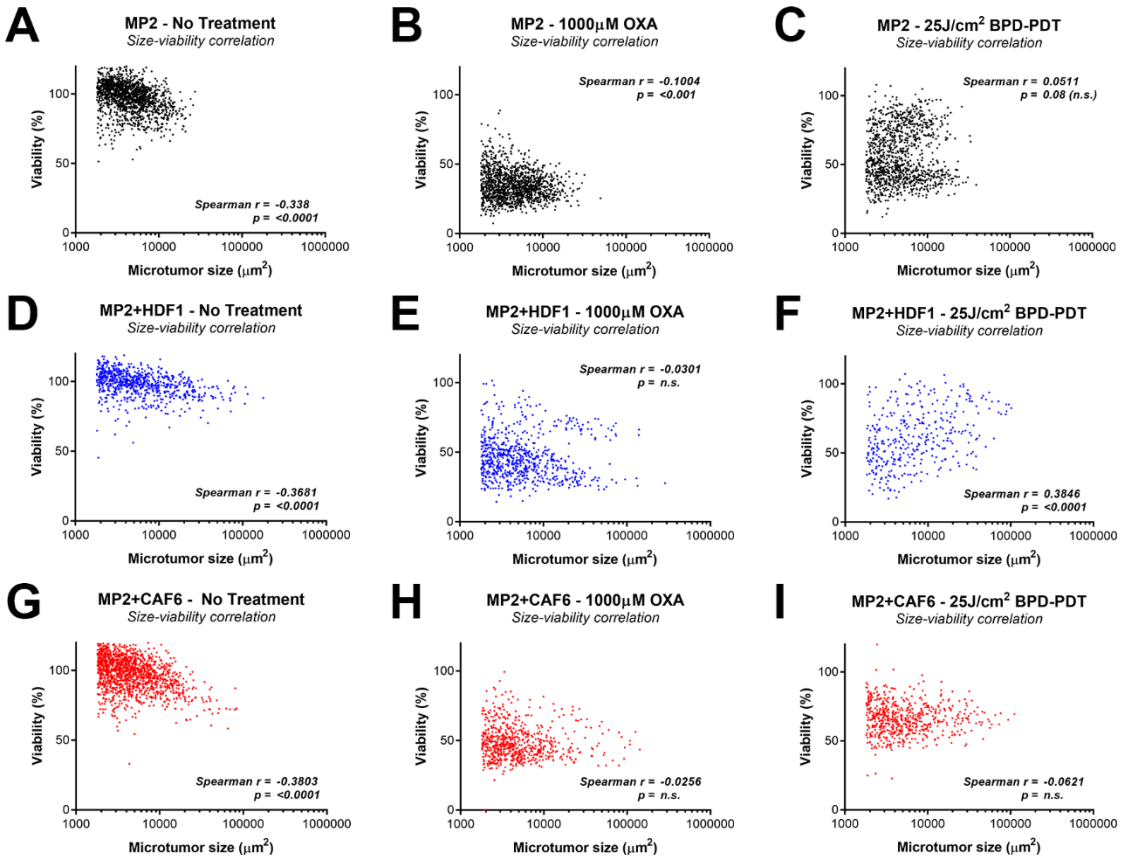

Figure S3. Correlation between microtumor size and treatment susceptibility. Microtumor viability was plotted as a function of their size for MP2 cultures **(A-C)**, MP2+HDF1 cultures **(D-F)**, and MP2+CAF6 cultures **(G-I)**, following no treatment **(A/D/G)**, 1000 µM oxaliplatin **(B/E/H)**, and 25 J/cm² BPD-PDT **(C/F/I)**. Data pointes were pooled from 3 technical repeats. Correlations were calculated using a Spearman rank test.

Figure S4.

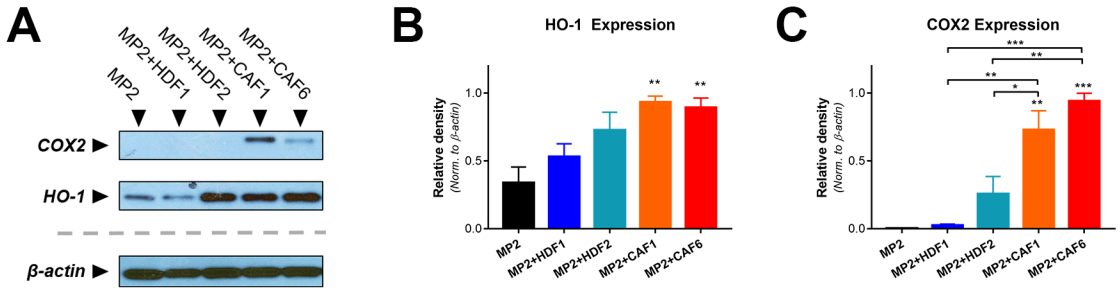

Figure S4. Evaluation of oxidative stress-induced survival protein expression in MP2 heterotypic microtumors. (A) Immunoblots of HO-1, COX2, and β-actin (loading control) expression. **(B)** Immunoblot quantification of HO-1 expression, normalized to the relative β-actin levels. Data represents mean ± SEM from ≥4 technical repeats, analyzed with a one-way ANOVA and a Holm-Sidak's multiple comparisons test. **(C)** Immunoblot quantification of COX2 expression, normalized to the relative β-actin levels. Data represents mean ± SEM from 3 technical repeats, analyzed with a one-way ANOVA and a Holm-Sidak's multiple comparisons test.

Figure S5.

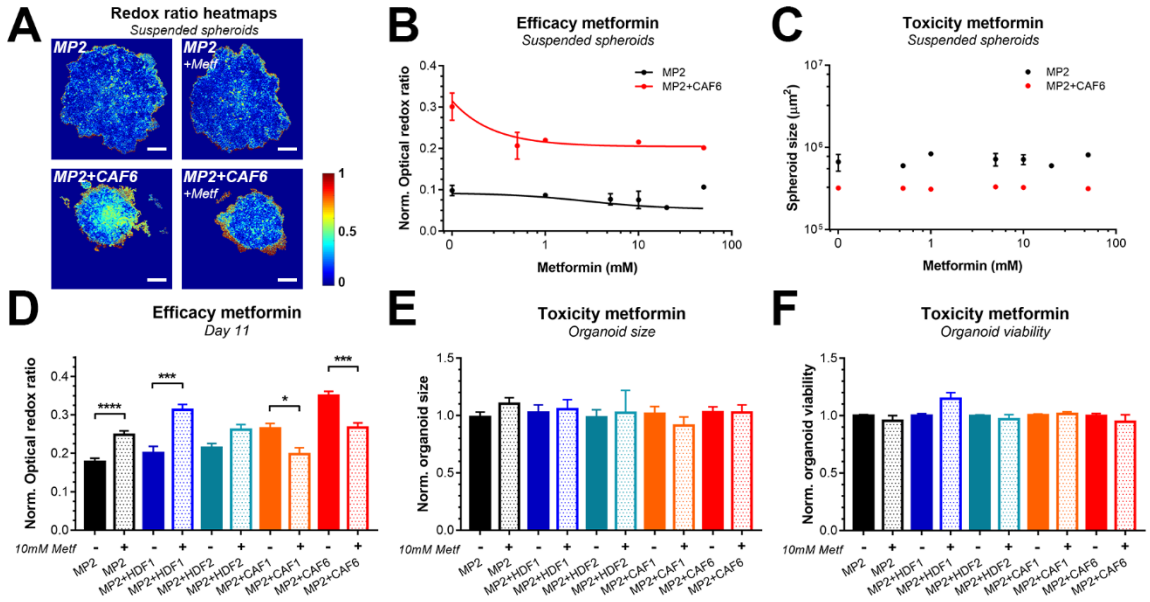

Figure S5: Metformin downmodulates redox states in 3D PDAC heterotypic cultures while exerting minimal toxicity. (A) Redox ratio heatmaps of 4 day-old MP2 and MP2+CAF6 spheroid cultures that were either untreated or exposed to 10 mM metformin for 48 h. **(B)** Dose-response correlation between spheroid redox states and metformin concentration, as determined on MP2 spheroids (black) or MP2+CAF6 spheroids (N = 1-3). **(C)** Toxicity of metformin comparing metformin dose to spheroid size (MP2 spheroids (black) or MP2+CAF6 spheroids (red), N = 1-3). **(D)** Quantification of redox states in adherent microtumor cultures of MP2 (black), MP2+HDF1 (blue), MP2+HDF2 (turquoise), MP2+CAF1 (orange), and MP2+CAF6 microtumors (red) on culture day 11, following a 48 h exposure to 10 mM metformin (median ± 95% CI of N = 56–252). **(E)** Effect of 10 mM metformin exposure (96 h) on overall microtumor size (median ± 95% CI of N = 12-32). **(F)** Effect of 10 mM metformin exposure (96 h) on overall microtumor viability (median ± 95% CI of N = 12-32).

Figure S6.

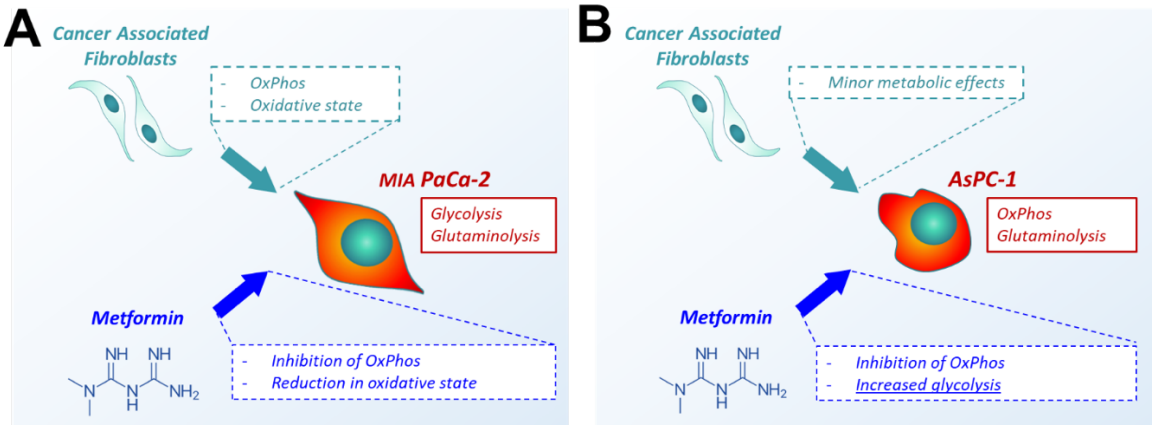

Figure S6: Schematic overview of metabolic modulation by CAFs and metformin in heterotypic PDAC microtumors. (A) Baseline metabolism of MP2-microtumors cells rely mostly on glycolysis and glutaminolysis, requiring minimal involvement of OxPhos. In presence of CAFs, microtumors display an increased OxPhos activity resulting in an increased oxidative state that can be mitigated by metformin. Baseline metabolism of AsPC-1 microtumors involves both OxPhos and glutaminolysis, resulting in higher oxidative states. The presence of CAFs in heterotypic AsPC-1-based microtumors leads to minimal metabolic alterations. Metformin impairs OxPhos and glutaminolysis in these microtumors, leading to a strong upregulation of glycolysis. However, oxidative states in AsPC-1-based microtumors is not perturbed

Figure S7.

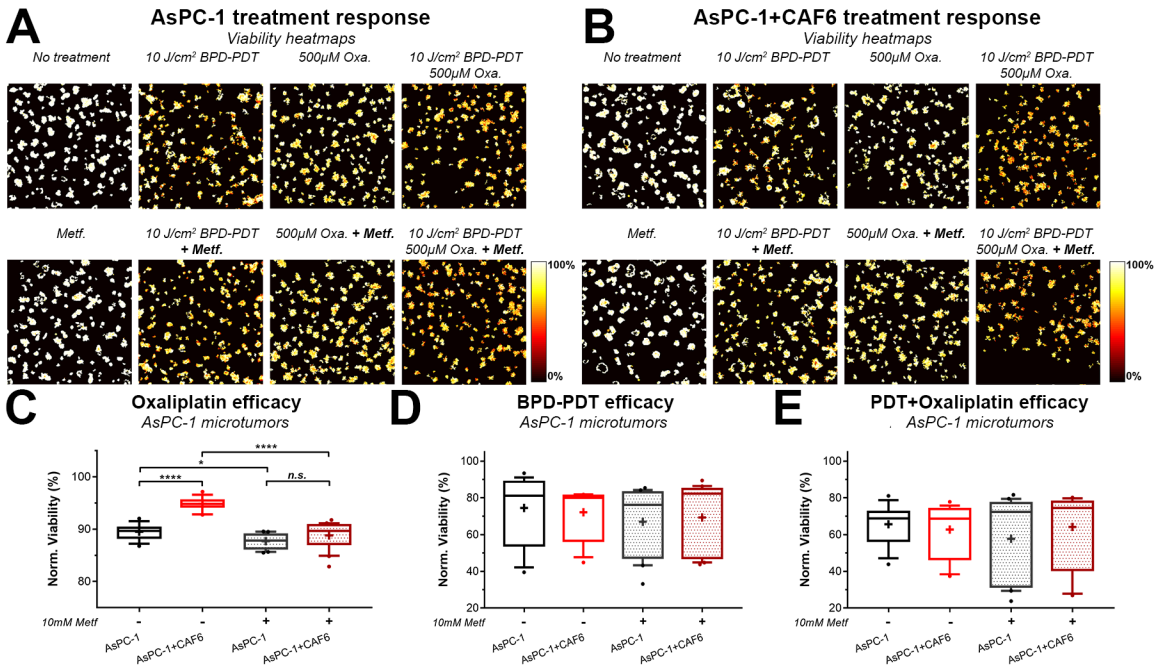

Figure S7. Inhibition of oxidative phosphorylation with metformin does not overcomes CAF6-induced treatment resistance in AsPC-1-based microtumors. (A) Viability heatmaps of AsPC-1 microtumors following treatments as indicated. **(B)** Viability heatmaps of AsPC-1 microtumors following treatments as indicated. **(C-E)** Box-whisker plots (median, mean, 90% CI, N = 18) depicting the viability of AsPC-1 and AsPC-1+CAF6 microtumor cultures following treatment with 500 µM Oxaliplatin +/- 10 mM Metf **(C)**, 10 J/cm^2 BPD-PDT **(D),** and a photochemotherapy of 10 J/cm^2 BPD-PDT and subsequent 500 µM oxaliplatin =/- 10 mM Metf. **(E)**.